SUPPORTING INFORMATION

Effects of Carbon Nanotube-Tethered Nanosphere Density on Amperometric Biosensing: Simulation and Experiment

Jonathan C. Claussen[1,2,3,†], James B. Hengenius[4,†],Monique M. Wickner[1,3], Timothy S. Fisher,[1,5] David M. Umulis[2,3,6,] D. Marshall Porterfield,[1,2,3,6,*]*

[1]Birck Nanotechnology Center, [2]Bindley Bioscience Center, [3]Department of Agricultural and Biological Engineering, [4]Department of Biological Sciences, [5]School of Mechanical Engineering, [6]Weldon School of Biomedical Engineering, Purdue University, West Lafayette, IN 47907

[†]Authors contributed equally to this work

*Corresponding authors' emails: dumulis@purdue.edu & porterf@purdue.edu

Computational Methods

Simulating biosensor current output. The total biosensor current is computed as a weighted sum of nanosphere currents simulated under different microenvironments; weights represent the fraction of nanospheres in each microenvironment multiplied by the total number of nanospheres. To compute the total number of nanospheres, we used the MATLAB Image Processing Toolbox®,[1] to analyze the FESEM images of the biosensor surface. The SWCNTs are not explicitly modeled because as compared to the Pt nanospheres, the exposed surface area of the SWCNTs is relatively small and the sidewalls of SWCNTs are generally considered

electrochemically inert except at defect sites or edge plane like sites,[2,3] and since these defects are most likely the nucleation sites for the subsequent Pt electrodeposition[4] the remaining exposed SWCNT is assumed to be electrochemically inactive.

Theoretical current output from low-density Pt nanosphere decorated SWCNTs. To simulate the current in electrodes, the finite element method (FEM) was utilized as implemented in COMSOL Multiphysics®, solving the system that modeled reaction-diffusion kinetics associated with distinct biofunctionalized Pt nanosphere electrodes. Initial physiochemical parameter values were obtained from the literature and were fixed whenever possible (see **Table S1**).

Table S1. Physiochemical Parameter Values

Parameter	Value	Units	Reference	(Lower Bound, Upper Bound)	Optimized Parameter
D_G	6.0×10^{-10} m^2s^{-1}	$[L^2/T]$	**5**	-	-
K_M	2 mM	$[m/L^3]$	Sigma-Aldrich	(2 mM, 30 mM)	24.9 mM
k_{cat}	1350 s^{-1}	1/[T]	**6**	-	-
E_{TOT}	8.2×10^{-6} $mmolm^{-2}$	$[m\ L^{-2}]$	Calculated	(1×10^{-10}mmol m^{-2}, 0.1 mmol m^{-2})	4.3861×10^{-6} $mmolm^{-2}$
V_{max}	$k_{cat}\ E_{TOT}$	$[m\ L^{-2}\ T^{-1}]$	Calculated	-	-
m, meters;	s, seconds;	mM, millimolar;	mmol, millimoles		
L, length;	T, time;	m, mass			

*Note: Dashes in columns signify parameters were fixed at literature values.

The value for E_{TOT} reported in **Table S1** represents an upper bound for enzyme density on the nanosphere surface. This upper bound was calculated by analyzing the footprint of GOx. A single GOx enzymatic dimer in natural conditions has a cross-sectional diameter of approximately 8 nm.[7] Assuming that the dimer is approximately spherical, it has a cross-sectional area of approximately 50 nm^2. The nanosphere has a diameter of 150 nm and a surface

area of approximately 70,000 nm^2. Dividing the surface area by the cross sectional area, we approximate the maximum number of GOx dimers per nanosphere at about 1400 or approximately 8.2×10^{-6} mmol m^{-2}.

Electrode density calculations via image analysis techniques. The approximate density and spacing of Pt nanospheres on the biosensor surface is acquired to more accurately simulate the current output for the entire biosensor. The experimental inter-Pt nanosphere distance data was best fit by an exponential function with a nearly equivalent mean (μ = 366 nm) and standard deviation (σ = 360 nm) and decay constant ($1/\mu$) (**Fig. 3c**). The distribution of defect sites along a finite length of CNT (thought to be nucleation sites for nanoparticle formation[4]) are Poisson distributed where the length of intervals between Poission-distributed nanospheres follows an exponential distribution. While most nanospheres have small inter-nanosphere distances and experience local glucose depletion (with a corresponding decrease in current), a few have no nearby neighbors and benefit from radial diffusion of glucose (with improved current).

We estimated the total number of nanospheres on the biosensor surface using FESEM images in conjunction with MATLAB's Image Processing Toolbox®. An unaltered top-view FESEM image of SWCNTs on the PAA surface (**Fig. S1a**) is converted to a binary matrix by determining threshold intensity, converting all pixels to zero or one if they fell above or below the respective threshold intensity. The connectivity of pixel clusters in the binary matrix was subsequently analyzed and all objects with fewer than ten pixels, which can be considered as noise, were discarded (**Fig. S1b**).

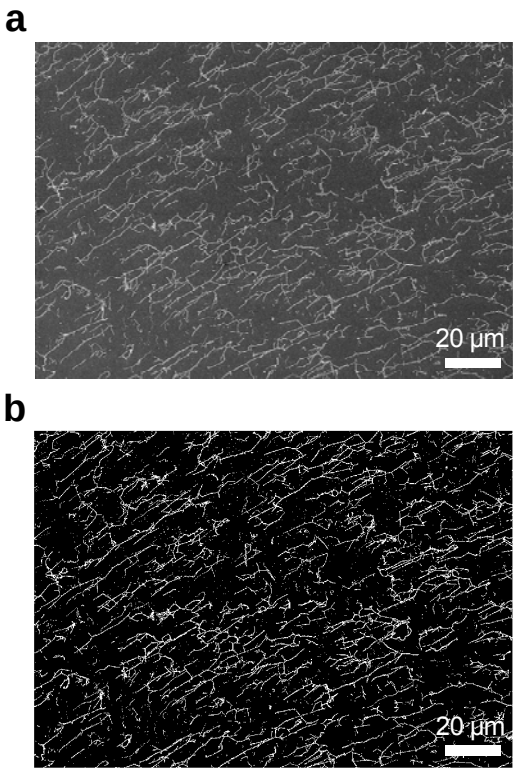

Fig. S1. FESEM image (**a**) is processed in MATLAB's Image Processing Toolbox® and converted to a filtered binary image (**b**). The area of metal coated SWCNTs is calculated as the fraction of white pixels on the image, multiplied by the total area of the image in square microns.

The ratio of white pixels to total pixels in the binary image is proportional to the SWCNT area on the image. We multiplied this fraction by the area of the image in square microns to determine the SWCNT area *A*. Assuming that all SWCNTs have a uniform width *w*, the total length *l* of the SWCNTs may be approximated as *A/w*. We measured the width *w* from the image to find the total SWCNT length *l* for the image. Because the image represented only a fraction of the 0.25 cm^2 biosensor surface, we scaled the SWCNT length appropriately to find the SWCNT length for the entire biosensor of approximately 7.32 m.

Theoretical current output from high-density Pt nanosphere decorated SWCNTs. In addition to the model for a biosensor with a low-density distribution of nanospheres, we constructed a model to simulate biosensor output when nanospheres are packed end-to-end along

SWCNTs. In the low-density nanosphere simulation, domains are used to approximate the distribution of microenvironments experienced by nanospheres. This approximation is not required in the simulation of a high-density Pt nanosphere/SWCNT biosensor. Because individual nanoelectrodes lie flush against adjacent nanoelectrodes in a high-density environment (**Fig. 5a**), all nanoelectrodes experience a similar spatial environment. We therefore use only a single model domain to simulate the total high-density nanosphere biosensor current. We do so by simulating a nanosphere with no inter-nanosphere space (*i.e.*, the nanosphere footprint is the diameter of the nanosphere without any adjacent exposed CNT) (**Fig. 2**).

REFERENCES

(1) *MATLAB version R2009b., The MathWorks Inc. (http://www.mathworks.com)* **2010**.

(2) Banks, C. E.; Compton, R. G. New Electrodes for Old: From Carbon Nanotubes to Edge Plane Pyrolytic Graphite. *Analyst* **2006**, *131*, 15.

(3) Banks, C. E.; Davies, T. J.; Wildgoose, G. G.; Compton, R. G. Electrocatalysis at Graphite and Carbon Nanotube Modified Electrodes: Edge-Plane Sites and Tube Ends Are the Reactive Sites. *Chem. Comm.* **2005**, *2005*, 829.

(4) Fan, Y.; Goldsmith, B. R.; Collins, P. G. Identifying and Counting Point Defects in Carbon Nanotubes. *Nat. Mater.* **2005**, *4*, 906.

(5) Weast, R. C.; Chemical Rubber, C. *Crc Handbook of Chemistry and Physics* **1988**; CRC press Boca Raton, FL, 1988.

(6) Karmali, K.; Karmali, A.; Teixeira, A.; Curto, M. J. M. Assay for Glucose Oxidase from Aspergillus Niger and Penicillium Amagasakiense by Fourier Transform Infrared Spectroscopy. *Anal. Biochem.* **2004**, *333*, 320.

(7) Rando, D.; Kohring, G. W.; Giffhorn, F. Production, Purification and Characterization of Glucose Oxidase from a Newly Isolated Strain of Penicillium Pinophilum. *Appl. Microbiol. Biot.* **1997**, *48*, 34.